analytical chemistry

pubs.acs.org/ac Technical Note

Fiber Probe for Simultaneous Mid-Infrared and Fluorescence Spectroscopic Analysis

Andrey Bogomolov, Tatiana Sakharova, Iskander Usenov, Camillo Mizaikoff, Valeria Belikova, Stanislav Perevoschikov, Viacheslav Artyushenko, and Olga Bibikova*

Cite This: https://doi.org/10.1021/acs.analchem.1c00080 Read Online

ACCESS | Metrics & More | Article Recommendations | Supporting Information

ABSTRACT: A multispectral fiber optic probe has been developed that enables simultaneous analysis of various liquid and solid samples using attenuated total reflection mid-infrared spectroscopy and fluorimetry. The probe design was optimized using ray-tracing simulation of the light propagation. Technical evaluation of the probe has confirmed its output signal quality that was comparable to that of respective probes for single methods. The capability of the probe to deliver complementary chemical information from the same measurement point has been illustrated using model samples of biological tissue. Qualitative analysis of the biological tissue is one of the most important applications of the developed multispectral probe.

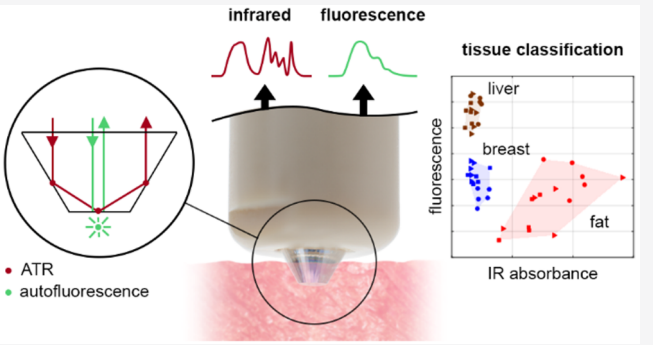

INTRODUCTION

Optical spectroscopy offers a number of flexible analytical techniques for studying the sample properties at the molecular level. Depending on the chosen spectral range and measurement geometry, optical spectra can deliver various chemical and morphological information about an object under study. Fiber optics and probes on its basis enable sampling-free measurements *in situ*, thereby essentially expanding the scope of optical analysis compared to the traditional lab spectroscopy.[1]

Modern applications of fiber-probe optical spectroscopy include in-line control of industrial processes,[2] field analysis in agriculture,[3] ecological monitoring,[4,5] and medical diagnostics.[6−8] Considerable progress in this area is associated with the advent of new optical fiber materials on the basis of chalcogenide glasses and polycrystalline silver halides[1,9] having sufficiently high transmittance in different intervals of the mid-infrared (IR) spectral region (4000−400 cm^{-1}). The modern optical fiber probes together cover the entire practical range of the optical spectroscopic analysis, thereby extending the applicability of ultraviolet, visible, near and mid-IR spectroscopy. They are designed to measure various effects of the light-to-sample interaction: absorbance, diffuse reflectance, attenuated total reflection (ATR), Raman scattering, and luminescence (in particular, fluorescence).[7,10,11]

The application of fiber optic probes can be moreover indispensable for the spectroscopic analysis of solid inhomogeneous samples, such as pharmaceutical and food products,[12] soils,[5] and biological tissues,[13] where focusing on the local analysis of the chemical composition is required. Our previous works have illustrated the feasibility of discrimination of human kidney[14,15] or colon[16] tumors using near-infrared (NIR), IR, and fluorescence spectroscopy as well as a LED-based sensor equipped with a fiber probe.[14] Although ATR spectroscopy is not optimal for the analysis of solid objects, its application for the analysis of biological tissues by fiber-based probes is one of the most important exceptions.[17]

For complex samples and challenging analytical tasks, any single spectroscopic technique can be insufficient for reliable analysis. Thus, in the case of tumor diagnostics, multiple chemical biomarkers and morphological changes of the tissue should be determined at a time to distinguish between the normal and malignant cells, especially near the border of the tumor. Preliminary investigations on the clinical samples have shown that optical diagnostics using a combination of fluorimetry with diffuse reflectance NIR[16] or ATR IR[15] spectroscopy results in much better accuracy of the tumor margin detection than each of the methods individually. This synergy was explained by the capability of methods to deliver complementary chemical information, i.e., indicate the presence of different tumor biomarkers. Whereas the superficial ATR analysis with its penetration depth of a few micrometers acts as the single-cell level, the ultraviolet−visible

Received: January 7, 2021
Accepted: March 15, 2021

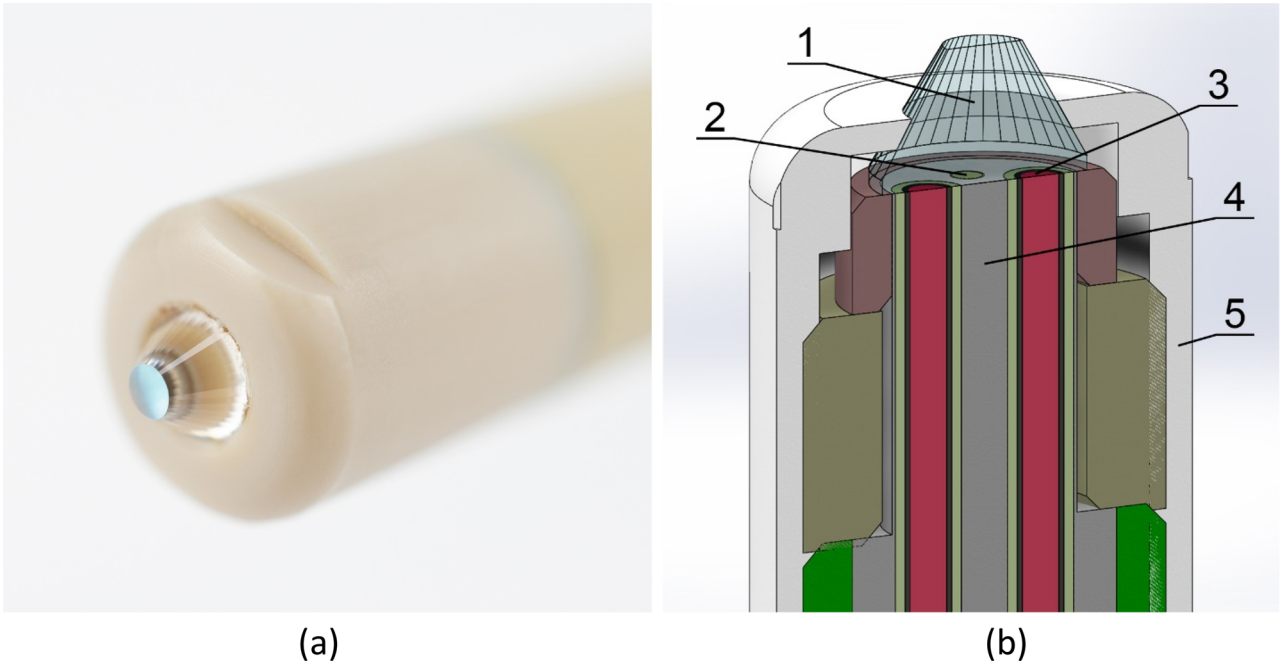

Figure 1. Multispectral probe head design: (a) the probe photo and (b) axial cross-section, where 1, ATR crystal; 2, silica fibers; 3, CIR fibers; 4, ferrule; and 5, probe shaft.

(UV−vis) light used in fluorimetry can penetrate to the depth of a few millimeters into the tissue[18] helping to detect the tumor border more reliably. The main challenge of such local multispectral analysis is related to the necessity to perform different spectroscopic measurements at the same point simultaneously. For instance, a marking grid was applied in a lab experiment[14] to ensure the compatibility of separate measurements on the same points using IR and fluorescence probes. Such alternating multispectral measurements cannot guarantee complete coincidence of the spots analyzed by both methods and, moreover, cannot be used in the clinical surgery practice.

The purpose of this study was to develop, assemble, and evaluate a multispectral fiber optic probe for the simultaneous analysis of test liquids and biological tissue samples by ATR IR spectroscopy and fluorimetry. The main problem to be solved in this case is the probe design, including the optimal measurement geometry and the choice of necessary materials in order to provide sufficient quality of the signals detected by each technique, despite the very different optical characteristics of the construction elements.

RESULTS AND DISCUSSION

Probe Design and Evaluation. Mid-IR spectroscopy and fluorimetry are very different in physical phenomena and wavelength ranges used for the chemical analysis, and therefore, their coupling within one probe is a challenging task. The proposed solution (Figure 1) is based on a precise determination of the optical configuration of the ATR crystal head, which, in this case, plays the role of a common measurement interface for both methods. ZrO_2 crystal was chosen due to its high (close to the diamond) refractive index, high transparency in the working spectral regions of both chalcogenide infrared (CIR) and UV silica fibers, as well as small intrinsic fluorescence.

The frustum geometry provides three total internal reflections of the IR light with a 60° angle of incidence instead of two reflections in a more common nontruncated cone with the light incidence at 45°. The total transmittance of IR light in this crystal calculated by the ray-tracing simulations (see the Supporting Information) was 19.0% and 17.2% for air and water, respectively. These are typical values for an ATR crystal of zirconium dioxide.

A round platform at the top of the truncated cone simultaneously serves to record fluorescence spectra. Silica fiber end faces are located exactly below it, providing the orthogonal sample illumination and reception of the fluorescence signal emitted back by the sample. At the same time, the CIR fiber cross sections are positioned right below the slopes of the cone beside its truncated apex (Figure 1 as well as Figures S-1 and S-2 in the Supporting Information). The diameters of two silica fibers and the distance between them were optimized for the fluorimetric analysis of a condensed-phase sample contacting the crystal tip of the probe. The frustum tip diameter of 1.1 mm was found to be optimal for the fluorescence measurement. The calculated total transmittance of the fluorescence channel was 70.4% for the air and 76.5% for the water medium.

The proposed crystal design[19] is particularly convenient for the analysis of liquid or soft solid samples, such as biological tissues. The most complete spectral information can be obtained by immersing the entire crystal element into the sample. The whole region simultaneously analyzed by both methods is within the circle formed by the base of the crystal cone, and the region of the most effective analysis is somewhat smaller. It has an elongated shape with the regions of IR and fluorimetric analysis equal to about 2 and 1 mm, respectively (Figure S-1b). Thus, the proposed crystal geometry is optimized for both measurements. The incomplete coincidence of the areas of analysis on the sample plays no significant role, if the spot under the measuring element is considered homogeneous. This requirement is easily fulfilled for a number of practical applications, e.g., for the analysis of biological tissue. Almost point analysis is performed, if the probe contact

https://doi.org/10.1021/acs.analchem.1c00080
Anal. Chem. XXXX, XXX, XXX−XXX

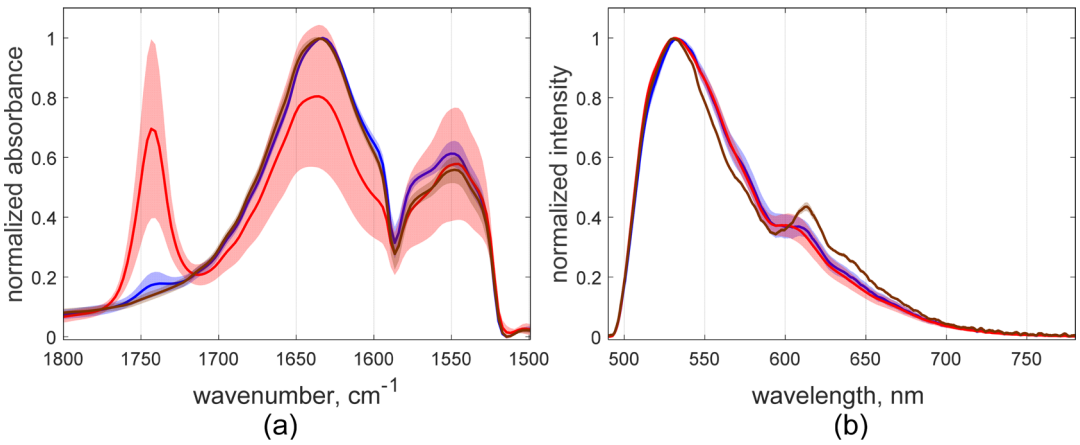

Figure 2. Normalized experimental spectra of chicken breast (blue), fat (red), and liver (brown) acquired with the multispectral probe: (a) IR spectra and (b) fluorescence spectra preprocessed by SNV. The curves and the surrounding colored regions represent the mean spectra and the standard deviation intervals of the respective data variables.

with the sample is limited to the flat crystal tip, although at the expense of a possible loss of IR signal intensity.

In the future, the probe size can be reduced to the critical diameter of 2 mm that is limited by the minimal thickness of CIR fibers, which enables endoscopic applications. ATR head and hence the spot of multispectral measurement can then be reduced to about 1 mm. The ATR crystal shape can also be modified to minimize the probe and to optimize the measured spot.

The comparison of multispectral probe with its single-method analogues using the standard isopropanol and fluorescein samples has shown good signal quality of the combined techniques (see Figure S-3 and discussion in the Supporting Information). The observed loss of intensity in the fluorescence channel is due to a smaller number of detection fibers, as dictated by the optimal geometry of the ATR crystal. No mutual influence of the combined spectroscopic methods was found. The probe design, construction, and technical evaluation was performed by art photonics GmbH (Berlin, Germany).

Multispectral Classification of Biological Tissue. The developed multispectral probe was tested in the practical analysis of biological tissue samples using different organs and parts of the chicken: breast, fat, and liver. The general chemical similarity of biological objects makes spectroscopic recognition of different tissue types a nontrivial task, which requires careful optimization of the measurement technique. Commercially produced poultry combines the availability of fresh samples and the variability of tissue types, making it an attractive model system for evaluating spectroscopic methods and equipment.

To provide the necessary statistical representativeness of the data, three samples of each tissue type were prepared. The samples were large enough to reflect the possible heterogeneity of the tissue. Each sample was represented by five distributed points. This experimental design resulted in two data matrices: a 45 × 118 $\mathbf{X}_{IR}$ matrix of Fourier-transform (FT) IR and 45 × 705 $\mathbf{X}_{FL}$ of fluorescence spectra (see the Supporting Information for more information).

Preliminary visual exploration of the obtained spectra (Figure 2) revealed the different abilities of the two techniques to recognize certain tissue types. The discriminative power of mid-IR spectroscopy (Figure 2a and Figure S-4) toward rich in lipids fat samples is related to the stretching vibration band of the ester carbonyl C═O at about 1740 cm^{-1}, which is characteristic of saturated triglycerides.[20] At the same time, all three sample types (fat to a lesser extent) have in the selected region two very similar signals with maxima at 1548 and 1640 cm^{-1}. These are, respectively, the amide I and II bands, two major absorption peaks of the protein peptide group in the infrared region.[21] Low measurement reproducibility of the fat samples (broad standard deviation in Figure 2a) is explained by higher inhomogeneity of this tissue type, because the spectra in all points of analysis always represent a mixture of lipids with an essential part of neighboring proteins. This fact also explains the presence of protein amide I and II bands in the IR spectra of fat in Figure 2a, making those bands less useful for the sample classification.

The fluorescence spectra (Figure S-5 in the Supporting Information) after standard normal variate (SNV)[22] correction look very similar below 600 nm (Figure 2b). Low standard deviations of the preprocessed spectra indicate homogeneity of the samples from the fluorimetric point of view (considering larger analyzed volumes). The observed broad band with the maximum between 520 and 530 nm is formed by the emission of intracellular fluorophores with the dominating contribution of flavin adenine dinucleotide (FAD)[23] that can be affected by the overlaying laser emission peak "tail" passed through the optical filter used (Supporting Information). This possible distortion, however, does not play any significant role in the sample classification. The most selective peak at 613 nm, which can be assigned to porphyrins, has sufficient specificity to distinguish the liver from other measured samples. The increased content of this protein in the liver is expected, since the liver has a central role in the metabolism of haem and porphyrins/porphyrinogens, which are intermediates in the haem biosynthetic pathway.[24]

Principal component analysis (PCA)[25] was used to evaluate the advantage of multispectral measurement with the developed probe for multivariate sample classification. IR and fluorescence data parts presented in Figure 2 were analyzed both separately and jointly without any further modification, thus enabling a direct comparison of the results. For the joint analysis, the IR and fluorescence spectra rescaled to have intensities between 0 and 1 were fused into a single matrix $\mathbf{X}$ (45 × 823) with the augmented spectral axis: $\mathbf{X} = [\mathbf{X}_{IR}\mathbf{X}_{FL}]$. The purpose of the data analysis was to investigate

https://doi.org/10.1021/acs.analchem.1c00080
Anal. Chem. XXXX, XXX, XXX−XXX

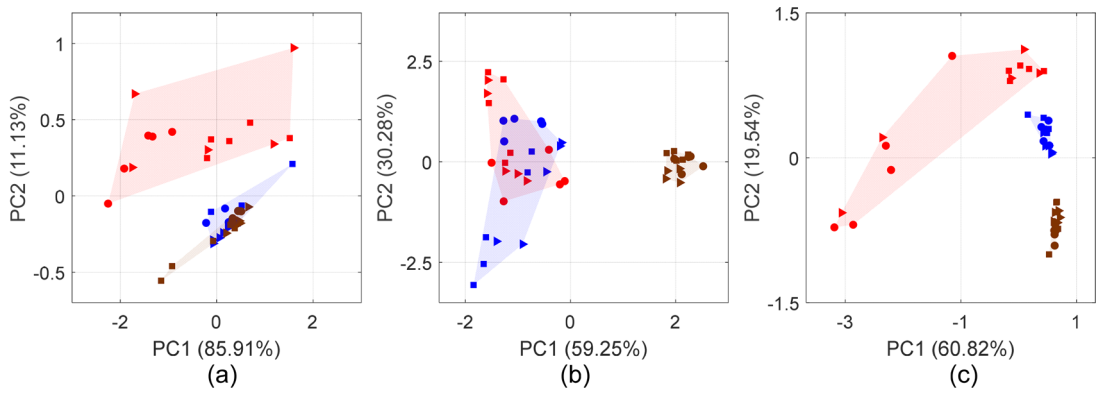

Figure 3. Score plots of the PCA models built for different data blocks of the multispectral analysis of chicken fat (red), breast (blue), and liver (brown): (a) IR spectra only, (b) fluorescence spectra only, and (c) combined data. Different marker types designate three different samples of the same tissue type.

the unsupervised clustering into three classes corresponding to the chicken tissue types. The scatter plots of the first two principal components (PCs) capturing the main spectral information in the data are presented in Figure 3.

PCA models for individual data blocks confirmed the above conclusions based on the spectral interpretation that IR spectroscopy works better for the discrimination of fat (Figure 3a), whereas fluorescence is well suited for the recognition of liver tissue (Figure 3b). However, none of the individual techniques was sufficient to completely separate the three sample classes on the PCA score plots (PCs one to five were investigated). At the same time, the PCA model built on the concatenated IR and fluorescence data revealed three distinct groups of samples corresponding to tissue types (Figure 3c). PCA loading plots (Figure S-6) reveal the importance of the above-discussed IR and fluorescence peaks for the tissue class separation in the PC1-PC2 plane and the effect of data concatenation on the variable weights in the model. The data preprocessing and analysis in this study were deliberately minimized to facilitate understanding of how complementary spectral information contributes into the joint multivariate model. If necessary, the models can be improved using supervised classification techniques, variable selection, and spectral transformations (e.g., derivatives), also using the entire available spectral range up to 4000 cm^{-1}.

This simple example illustrates the gain that can be obtained using the proposed multispectral probe in the qualitative analysis of biological tissue. The same effect can potentially be observed in various real-life applications, such as medical diagnostics. The synergic effect of combining IR and fluorescence spectroscopy in the point-by-point recognition of kidney tumor shown in our earlier work[15] is expected to be strengthened due to a better spatial precision of the simultaneous multispectral measurement (compared to two individual probes) resulting in a more accurate determination of the tumor margin.

Although the presented multisensor probe was inspired by the analysis of biological samples, it has a broader scope of potential applications. Of course, it is limited to the samples containing at least one fluorescent component that often has a biological or natural origin. In addition to biological liquids and tissues, they include, for example, many vegetable products, mineral oils, and their derivatives. Another requirement is the suitability of analyzed samples for ATR measurements, which is true for liquid or soft solid samples and their components, allowing a tight contact with the probe head. Solid samples are typically represented by nonhomogeneous mixtures having complex matrixes with water (or another liquid component) as the major constituent. In fact, any spectral analysis of fluorescing mixtures suitable for ATR measurement can benefit from adding vibrational signals of the component molecules and vice versa.

The main focus of the proposed technology is on analyzing nonhomogeneous solid samples, because it enables simultaneous measurements at the same point on the sample surface. The proven ability of combined fluorimetry and ATR IR spectroscopy to detect the tumor boundary[15] is expected to have an impact on the oncological diagnostics. Optical methods are increasingly used in this practically important area, and the suggested technical approach becomes just indispensable here, because any sequential measurements in the same point using separate probes can hardly be done in practice, e.g., in clinical surgery.

Toward the Sensor System. One of the main disadvantages of the multispectral analysis limiting its wide dissemination is the use of two separate spectrometers to register IR and fluorescence spectra. This can be avoided in multisensor systems, where specialization for a particular application enables a technological simplification of the spectroscopic methods so that they can be combined in one compact analytical device. The developed concept of combining infrared and fluorescence spectroscopy provides a viable solution for the measurement interface in a multisensor system of this kind. The potential of limiting the analysis to only two relevant information channels is illustrated in Figure 4, where the full separation of different types of the chicken tissue was achieved on a plane of two spectral variables, one of each spectral method, whereas either single variable cannot classify them all. The fluorimetry can be adjusted to a particular application by choosing an appropriate excitation wavelength. Further development of the probe may include its modification to enable diffuse reflectance UV−vis and NIR measurements instead of the fluorimetry, thus opening new application areas.

CONCLUSION

A conceptually new approach to combining CIR and silica fibers in a single probe head has been developed.[19] It was used to construct a multispectral fiber optic probe that successfully solves the problem of simultaneous analysis (at the same time

https://doi.org/10.1021/acs.analchem.1c00080
Anal. Chem. XXXX, XXX, XXX−XXX

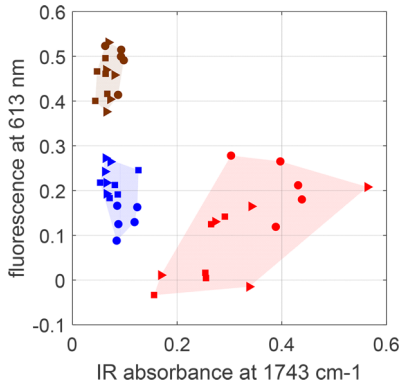

Figure 4. Multispectral probe measurements of chicken fat (red), breast (blue), and liver (brown) presented in the coordinate plane of two single-variable intensities of normalized spectra presented in Figure 2: IR absorbance at 1743 cm^{-1} and fluorescence at 613 nm. Different markers designate three different samples of the same tissue type.

and point) using ATR IR and fluorescence spectroscopy. Multispectral probes of this family are highly practicable and can be indispensable for the local analysis of complex heterogeneous samples, such as biological tissue, when combining spectroscopic techniques results in a synergic effect. The developed probe provides a well suited measurement interface for low-cost multisensor systems optimized for various particular applications as an alternative to the universal lab spectroscopy.

■ ASSOCIATED CONTENT

Supporting Information

The Supporting Information is available free of charge at https://pubs.acs.org/doi/10.1021/acs.analchem.1c00080.

Additional information on the probe design, sample preparation, spectral data acquisition and analysis, probe evaluation and used software (PDF)

■ AUTHOR INFORMATION

Corresponding Author

Olga Bibikova − *art photonics GmbH, Berlin 12489, Germany;* orcid.org/0000-0002-1929-7698; Email: ob@artphotonics.de

Authors

Andrey Bogomolov − *Samara State Technical University, 443100 Samara, Russia;* orcid.org/0000-0002-4832-638X

Tatiana Sakharova − *art photonics GmbH, Berlin 12489, Germany*

Iskander Usenov − *art photonics GmbH, Berlin 12489, Germany; Technische Universität Berlin, Institute of Optics and Atomic Physics, 10623 Berlin, Germany*

Camillo Mizaikoff − *art photonics GmbH, Berlin 12489, Germany*

Valeria Belikova − *Samara State Technical University, 443100 Samara, Russia*

Stanislav Perevoschikov − *Skolkovo Institute of Science and Technology, Moscow 121205, Russia*

Viacheslav Artyushenko − *art photonics GmbH, Berlin 12489, Germany*

Complete contact information is available at: https://pubs.acs.org/10.1021/acs.analchem.1c00080

Notes

The authors declare no competing financial interest.

■ ACKNOWLEDGMENTS

Authors from SSTU received funding from the Ministry of Education and Science of the Russian Federation within the framework of State Task No. 0778-2020-0005. Mestrelab Research is acknowledged for providing TPT-cloud software supported by the Project "Laboratorio Dixital do Futuro (FutureLab)" (IN854A 2019/16) funded by the Axencia Galega de Innovación (GAIN), through the Programa Industrias do Futuro 4.0 (terceira convocatoria) and cofinanced by the European Regional Development Fund (ERDF) (Cofinanciado con cargo aos fondos FEDER) under the Feder Galicia 2014−2020 Operational Program. It also has the support of the Consellería de Economía, Emprego e Industria. Ivan Bogomolov is acknowledged for graphics design.

■ REFERENCES

(1) Artyushenko, V.; Bocharnikov, A.; Colquhoun, G.; Leach, C.; Lobachev, V.; Sakharova, T.; Savitsky, D. *Vib. Spectrosc.* **2008**, *48*, 168−171.

(2) Bogomolov, A. *Chemom. Intell. Lab. Syst.* **2011**, *108*, 49−63.

(3) Shapira, U.; Herrmann, I.; Karnieli, A.; Bonfil, D. J. *Int. J. Remote Sens.* **2013**, *34*, 6094−6108.

(4) Jakusch, M.; Mizaikoff, B.; Kellner, R.; Katzir, A. *Sens. Actuators, B* **1997**, *38*, 83−87.

(5) Guryanova, A.; Ermakov, V.; Galyanin, V.; Artyushenko, V.; Sakharova, T.; Usenov, I.; Bykov, D.; Bogomolov, A. *J. Chemom.* **2017**, *31*, e2826.

(6) Ahn, H.; Song, H.; Shin, D. M.; Kim, K.; Choi, J. R. *Appl. Spectrosc. Rev.* **2018**, *53*, 264−278.

(7) Utzinger, U.; Richards-Kortum, R. R. *J. Biomed. Opt.* **2003**, *8*, 121−147.

(8) Mackanos, M. A.; Contag, C. H. *Trends Biotechnol.* **2010**, *28*, 317−323.

(9) Heise, H. M.; Küpper, L.; Butvina, L. N. *Sens. Actuators, B* **1998**, *51*, 84−91.

(10) Bogomolov, A.; Heßling, M.; Wenzel, U.; Princz, S.; Hellmuth, T.; Bernal, M. J. B.; Sakharova, T.; Usenov, I.; Artyushenko, V.; Meyer, H. *Sens. Actuators, B* **2015**, *221*, 1601−1610.

(11) Hanifi, A.; Bi, X.; Yang, X.; Kavukcuoglu, B.; Lin, P. C.; DiCarlo, E.; Spencer, R. G.; Bostrom, M. P.; Pleshko, N. *Am. J. Sports Med.* **2012**, *40*, 2853−2861.

(12) Schmitt, S.; Garrigues, S.; de la Guardia, M. *Crit. Rev. Anal. Chem.* **2014**, *44*, 186−197.

(13) Dong, L.; Sun, X.; Chao, Z.; Zhang, S.; Zheng, J.; Gurung, R.; Du, J.; Shi, J.; Xu, Y.; Zhang, Y.; Wu, J. *Spectrochim. Acta, Part A* **2014**, *122*, 288−294.

(14) Bogomolov, A.; Zabarylo, U.; Kirsanov, D.; Belikova, V.; Ageev, V.; Usenov, I.; Galyanin, V.; Minet, O.; Sakharova, T.; Danielyan, G.; Feliksberger, E.; Artyushenko, V. *Sensors* **2017**, *17*, 1914.

(15) Bogomolov, A.; Belikova, V.; Zabarylo, U. J.; Bibikova, O.; Usenov, I.; Sakharova, T.; Krause, H.; Minet, O.; Feliksberger, E.; Artyushenko, V. *Sensors* **2017**, *17*, 2548.

(16) Ehlen, L.; Zabarylo, U. J.; Speichinger, F.; Bogomolov, A.; Belikova, V.; Bibikova, O.; Artyushenko, V.; Minet, O.; Beyer, K.; Kreis, M. E.; Kamphues, C. *J. Surg. Res.* **2019**, *242*, 349−356.

(17) Ring, A.; Schreiner, V.; Wenck, H.; Wittern, K. P.; Küpper, L.; Keyhani, R. *Skin. Res. Technol.* **2006**, *12*, 18−23.

(18) Tuchin, V. V. *Tissue Optics: Light Scattering Methods and Instruments for Medical Diagnostics*, 2nd ed.; SPIE Press: Bellingham, WA, 2008.

(19) Artyushenko, V.; Sakharova, T.; Usenov, I.; Bogomolov, A.; Starodubov, D. *Diagnostic System with Multispectral Optical Fiber Probe*. Provisional U.S. Patent Application 63153426, 2021.
(20) Chapman, D. *J. Am. Oil Chem. Soc.* **1965**, *42*, 353−371.
(21) Baker, M. J.; Hussain, S. R.; Lovergne, L.; Untereiner, V.; Hughes, C.; Lukaszewski, R. A.; Thiéfin, G.; Sockalingum, G. D. *Chem. Soc. Rev.* **2016**, *45*, 1803−1818.
(22) Naes, T.; Isaksson, T.; Fearn, T.; Davies, T. A. *User Friendly Guide to Multivariate Calibration and Classification*, 1st ed.; NIR Publications: Chichester, U.K., 2002.
(23) Kotaki, A.; Yagi, K. *J. Biochem.* **1970**, *68*, 509−516.
(24) Bloomer, J. R. *J. Gastroenterol. Hepatol.* **1998**, *13*, 324−329.
(25) Wold, S.; Esbensen, K.; Geladi, P. *Chemom. Intell. Lab. Syst.* **1987**, *2*, 37−52.

https://doi.org/10.1021/acs.analchem.1c00080
Anal. Chem. XXXX, XXX, XXX−XXX